PHYSOR 2012 – Advances in Reactor Physics – Linking Research, Industry, and Education
Knoxville, Tennessee, USA, April 15-20, 2012, on CD-ROM, American Nuclear Society, LaGrange Park, IL (2012)

QUALIFICATION OF CASMO5 / SIMULATE-3K AGAINST THE SPERT-III E-CORE COLD START-UP EXPERIMENTS

Gerardo Grandi and Lars Moberg
Studsvik Scandpower, Inc.
504 Shoup Ave, Suite # 201, Idaho Falls, ID, 83402 USA
Gerardo.Grandi@studsvik.com; Lars.Moberg@studsvik.com

ABSTRACT

SIMULATE-3K is a three-dimensional kinetic code applicable to LWR Reactivity Initiated Accidents. S3K has been used to calculate several international recognized benchmarks. However, the feedback models in the benchmark exercises are different from the feedback models that SIMULATE-3K uses for LWR reactors. For this reason, it is worth comparing the SIMULATE-3K capabilities for Reactivity Initiated Accidents against kinetic experiments.
The Special Power Excursion Reactor Test III was a pressurized-water, nuclear-research facility constructed to analyze the reactor kinetic behavior under initial conditions similar to those of commercial LWRs. The SPERT III E-core resembles a PWR in terms of fuel type, moderator, coolant flow rate, and system pressure. The initial test conditions (power, core flow, system pressure, core inlet temperature) are representative of cold start-up, hot start-up, hot standby, and hot full power. The qualification of S3K against the SPERT III E-core measurements is an ongoing work at Studsvik. In this paper, the results for the 30 cold start-up tests are presented. The results show good agreement with the experiments for the reactivity initiated accident main parameters: peak power, energy release and compensated reactivity. Predicted and measured peak powers differ at most by 13%. Measured and predicted reactivity compensations at the time of the peak power differ less than 0.01 $. Predicted and measured energy release differ at most by13%.
All differences are within the experimental uncertainty.

Key Words: RIA Analysis, CRDA Analysis, SIMULATE-3K, CASMO5, SPERT-III E-core

1. INTRODUCTION

SIMULATE-3K (S3K) was designed to be a best estimate tool employing a full two-group advanced nodal method for the core neutronics. It is well suited for the analysis of Reactivity Initiated Accidents (RIA) in Light Water Reactors (LWR) [1-3]. S3K has been used to calculate the OECD/NEA REA benchmark [4-5], the OECD/NEA uncontrolled rod withdrawal benchmark [6-7] and the LMW benchmark [8]. However, the feedback models in the benchmark exercises (e.g. the cross section data, the Doppler temperature definition, the heat transfer package, to mention a few) are different from the feedback models that S3K uses for LWR reactors. For this reason, it is worth comparing the S3K capabilities against kinetic experiments. Our main intention is to validate the Studsvik codes CASMO5 and S3K for RIA under prompt transient conditions.

The Special Power Excursion Reactor Test III (SPERT III) was a pressurized-water, nuclear research facility constructed to analyze the reactor's kinetic behavior under initial conditions similar to those of commercial LWRs [9-10]. The SPERT III E-core, except for its size, resembles a PWR in terms of fuel type (oxide pellet type), moderator, coolant flow rate, and system pressure. The initial test conditions were representative of cold start-up, hot start-up, hot standby, and hot full power.

The qualification of S3K against the SPERT III E-core measurements is an ongoing work at Studsvik. This paper presents the results for 30 cold start-up tests in terms of peak power, compensated reactivity, energy release and overall behavior of the reactor power.

Section 2 provides a short description of the S3K neutronic, core thermal-hydraulic and fuel pin models. A brief description of the SPERT III E-core is provided in Section 3. Section 4 describes the applied CASMO5 / SIMULATE-3K model. Section 5 presents key results of the numerical simulations. Finally, conclusions are drawn in Section 6.

2. SIMULATE-3K DESCRIPTION

S3K is a nodal reactor kinetics tool that employs advanced core neutronics coupled with detailed thermal-hydraulic channel models. Faithful modeling of assembly-by-assembly neutronic and thermal-hydraulic effects, including assembly pin power reconstruction, permits application of S3K to a wide class of LWR core transients. Belblidia *et al*. [11] describes the core neutronic and the thermal-hydraulic channel in detail; while Grandi *et al*. [12] provides a detailed description of the fuel pin model. A brief summary of these models follows.

2.1 Core Model

The neutronic model used in S3K solves the transient three-dimensional (3D), two-group neutron diffusion equations, including a six-group model for delayed neutron precursors. The basic spatial integration model of S3K is formed via transverse integration of the 3D equations separately over each spatial direction. This procedure creates an equivalent set of three one-dimensional equations coupled via a transverse leakage term. The flux distribution is expanded in terms of fourth-order polynomials for the epithermal flux and analytical functions for the thermal flux in each direction and thus the spatial gradient of the flux can be analytically represented. The frequency transform method is used for the time integration. This method separates the flux into two components, one with a pure exponential time dependence, and the other with primarily spatial (and weak temporal) dependence. The frequency transform method is especially suitable for the analysis of RIAs.

2.2 Hydraulic Channel Model

The core is represented with one thermal-hydraulic channel per fuel bundle with no cross flow. The hydraulic model uses a five-equation model: vapor and liquid mass conservation, vapor and liquid energy conservation, and averaged momentum conservation. In addition to the conservation equations, closure relationships exist for each phasic density, defined as a function of the pressure and phasic enthalpy. Steam/water properties are evaluated at the core exit pressure. The general drift flux formulation for the void fraction completes the set of equations to be solved. The concentration parameter and the void-weighted drift velocity are calculated using the EPRI correlations. The subcooled boiling model is taken from Lahey’s mechanistic model.

2.3 Fuel Pin Model

The heat conduction in the fuel pin is governed by the one-dimensional, radial heat conduction equation. S3K takes into account the fact that fission energy is deposited both inside the fuel pellet and outside the pellet due to neutron slowing down and gamma attenuation. The radial distribution of the volumetric heat

source within the pellet is dependent on the fuel depletion. The radial distribution of the heat source is evaluated based on the pellet average exposure by interpolating in pre-computed tables generated with CASMO5 [13]. Fuel thermal conductivity for UO_2 depends on temperature and burnup. The S3K gap conductance model is functionalized against exposure and fuel temperature. The heat transfer coefficient between the wall and the coolant is determined from one of several different possible modes of heat transfer according to a classical boiling formulation.

3. DESCRIPTION OF THE SPERT III E-CORE

The SPERT III E-core is a small, oxide fueled PWR, which has the general characteristics of a commercial plant (except for its size) and with no fission product inventory. The design characteristics of the E-core are presented in Appendix A. The rated power is 20 MW, the rated flow 1.26 m^3/s and the design pressure and temperature are 17.33 MPa at 616 K. The E-core is composed of 4.8% enriched UO_2 fuel rods placed in stainless steel fuel assembly cans [10]. The active fuel length is 97.28 cm. The E-core has 60 fuel assemblies as shown in Fig. 1.

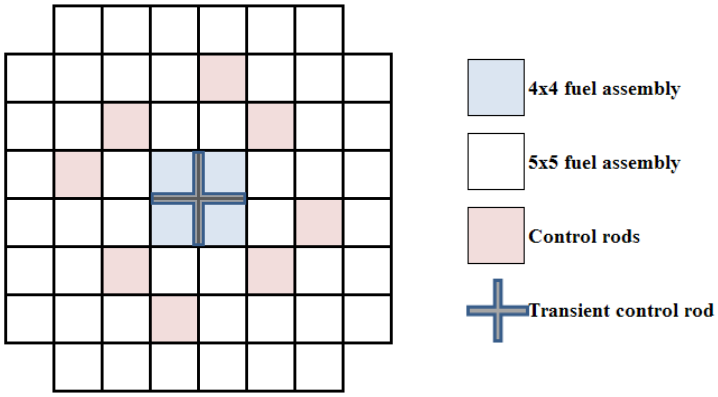

Figure 1. SPERT-III E-core.

The majority of fuel rods are contained in 48 fuel assemblies that are 7.62 × 7.62 cm square [10]. These assemblies contain 25 rods in a 5×5 square array with a 1.486 cm pitch. There are 12 smaller fuel assemblies that are 6.35×6.35 cm square [10]. Each of these smaller assemblies contains 16 fuel rods arranged in a 4×4 square array with the same pitch as the 25-rod assemblies. Four of the 16-rod assemblies surround the centrally located transient control rod guide and the remaining eight form fuel followers of the eight E-core control rods. The poison section of the control rod assemblies is constructed of stainless steel plate containing 1.35 wt% ^{10}B [10]. The UO_2 fuel, in the form of 1.067 cm diameter pellets, is contained in type 348 stainless steel tubes that are 103.632 cm long, with a 1.184 cm outside diameter and a wall thickness of 0.051 cm [10]. The cruciform-shaped transient control rod used for initiating the reactor power excursion is located at the core center (Fig. 1). The transient control rod also contains two sections. The lower absorber section is made of 1.35 wt% ^{10}B in type 18-8 stainless steel. The blade thickness is 0.476 cm and has a width of 13.0175 cm. The upper section is AISI Type 347 stainless steel. The upper section is normally in the core. The inserted reactivity for the RIA experiments is determined from the relationship between the transient control rod position and other control rod positions. In preparation for a power excursion the control rod assemblies are withdrawn to the desired position and the reactor is maintained critical by inserting the poison section of the transient control rod into the lower part of the core.

4. CASMO5 / SIMULATE-3K MODEL

The S3K model explicitly represents each of the 60 fuel assemblies. The chosen spatial discretization is: radial mesh of 1 node-per-assembly (Δx= 7.5570 cm) and 52 axial nodes (Δz=1.8708 cm). The fuel temperature (for the purpose of reactivity feedback) is calculated in a fictitious average power rod for each node. The pellet is divided into 10 regions of equal volume; one region represents the gaseous gap and the cladding is discretized into 2 regions. Due to the cruciform control rod, the E-core has been modeled as a Boiling Water Reactor (BWR) with three different fuel types. All nuclear data (two-group macroscopic cross sections, assembly discontinuity factors and kinetic parameters[*]) were calculated with CASMO5, for four different compositions: the 5×5 rods fuel (Fig. 2-a), the 4×4 rods fuel surrounding the transient control rod (Fig. 2-b), the upper section (poison) of the control rod assemblies and the lower section (fuel follower) of the control rod assemblies (Fig. 2-c and 2-d).

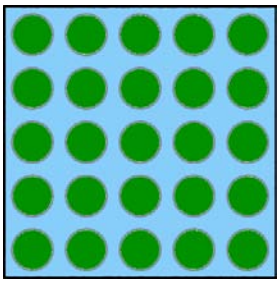

(a) 5x5 Fuel Assembly

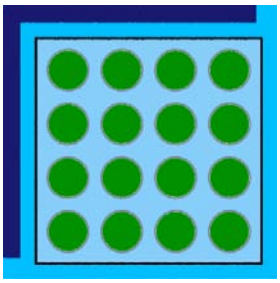

(b) 4x4 Fuel Assembly

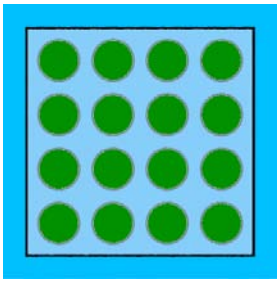

(c) Control Rod Assembly: lower part – fuel follower

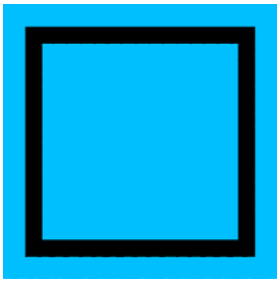

(d) Control Rod Assembly: upper part – ^{10}B absorber section

Figure 2. Fuel assembly models for the E-core.

All compositions were modeled as Pressurized Water Reactor (PWR) lattices. The dimensions required for the CASMO5 calculations are provided in Appendix A. Although the SPERT III reactor has no burnup history, the data was created at two burnup states (0 and 1 GWd/T). Calculations were performed at:

- Pressure 0.10132 MPa (atmospheric pressure)
- Coolant temperatures of 293 K, 313 K, 333 K, and 353 K
- Coolant temperature of 373 K and five states of instantaneous void, 0%, 20%, 40%, 60% and 80%
- Fuel temperatures of 293 K, 490 K and 1,500 K

[*] CASMO-5 delayed neutron fractions are not based on ENDF/B VII.0 data, but on the data used by CASMO-4.

The Doppler temperature effect in a thermal reactor is driven by ^{238}U absorption. There is considerable spatial self-shielding of the ^{238}U absorption and much of the absorption occurs near the surface of the fuel pin, where the temperatures are lowest. CASMO5 calculations assume that the temperature profile across a fuel pin is spatially flat. Therefore, S3K must calculate an "effective Doppler temperature," from the fuel temperature spatial distribution within the pin, such that the Doppler feedback is properly accounted for. The Doppler temperature (T_{DOP}) is computed as a weighted average of the volume-averaged temperature (T_A), and the fuel surface temperature (T_S),

$$T_{DOP} = \omega \cdot T_A + (1-\omega) \cdot T_S \tag{1}$$

where the volume-averaged temperature is defined by

$$T_A = \int T(r) \cdot r \cdot dr \Big/ \int r \cdot dr \tag{2}$$

The value of ω has been empirically adjusted (ω = 0.92) [14].

5. RESULTS

The cold start-up reactivity accident tests were all performed from a low initial power[†] and a system pressure of 0.101 MPa (atmospheric pressure). The initial system temperature was set to 294.3 K (21.1 ºC). The experiments were performed at zero mass flow but S3K cannot simulate such an experimental condition. For the purpose of the simulations, the initial power was set to 50 W and the flow was assigned a small value (~1 kg/s).

Fig. 3 summarizes the integral rod worth calculations for the 8 control rods in the operational core.

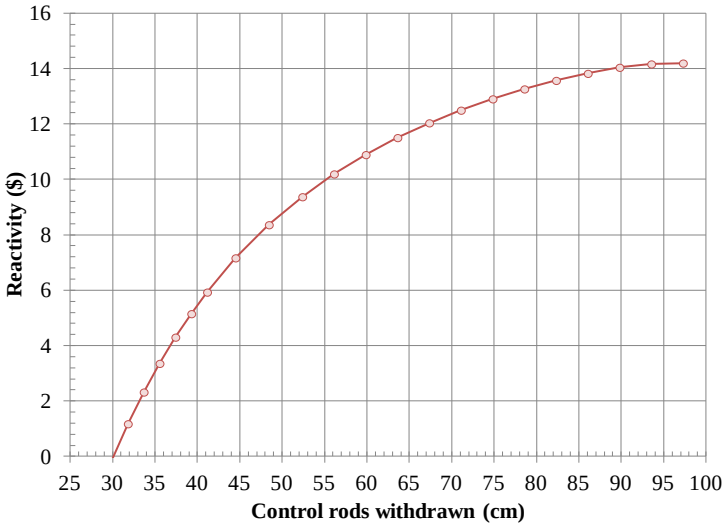

Figure 3. SPERT III E-Core integral control rod worth.

[†] The initial power for each of the tests is not provided in reference [10]

The operational core has a measured reactivity excess of 14.20 $. The reactor was critical with approximately 36.8 cm of the control rod poison section withdrawn. The calculated reactivity excess is 14.19 $ and the reactor is critical with 30.1 cm of the control rod poison section withdrawn. For the purpose of the transient simulations, it was assumed that the reactor was critical at 30.1 cm.

The transients were initiated with a rapid reactivity insertion varying from 0.77$ to 1.21$ for the different tests. When the transient control rod in the central position is ejected, its initial position basically determines the reactivity insertion. Unfortunately, the initial positions of the four control rods and of the transient control rod were not specified in reference [10]; only the reactor state, initial reactor period and initial reactivity insertion were specified. Therefore, the first step in the analysis was to position the transient control rod such that its static reactivity worth matches the reported initial reactivity. Meanwhile, the four control rods (with fuel followers) were moved to preserve the criticality in the core. The power excursion was initiated by ejecting the transient control rod from the core.

5.1. Initial Reactivity Insertion and Reactor Period

Table I compares the initial reactivity insertions provided in reference [10] and the actual reactivity insertions used in the S3K simulations. The uncertainty of the measurements is 0.04$. The initial measured reactivity is well matched in all cases. Differences are below 0.01$ in all cases; well within the uncertainty of the measurements.

In the cold start-up tests, the power increases several decades before any reactivity feedback effect comes into play. The reactor periods were measured during this initial phase of exponential growth and constitute a good characterization of the tests. Fig. 4 and Table I compare the measured and calculated reactor periods. Fig. 4-a shows measured (blue line) and calculated (red line) reactor periods as well as the differences (green line) for the different tests. For the purpose of the analysis, the cold tests may be divided into three sets:

- Cases with a reactor period greater than 0.200 s: Tests 22 – 14 belong to this category. These cases are sub-prompt critical. The inserted reactivity is below 0.97$. Test 14 is representative of this set with an inserted reactivity of 0.934$.
- Cases with a reactor period lower than 0.030 s: Tests 75 – 43 belong to this category. These cases are super-prompt critical. The inserted reactivity is above 1.03$. Test 43 is representative of this group with an inserted reactivity of 1.207$.
- Cases with a reactor period between 0.030 s and 0.200 s: Tests 30 – 20 belong to this category. These cases are close to prompt critical; the inserted reactivity is in the range of 0.97$ to 1.03$. Test 49 is representative of this set with an inserted reactivity of 1.006$. These cases are difficult to simulate because the uncertainty in the initial reactivity may change the case from sub-prompt critical to super-prompt critical.

Table I: Initial reactivity insertion and reactor period.

Test No.	Initial Reactivity ($)			Reactor Period (ms)		
	SPERT	S3K	Diff.	SPERT	S3K	Diff.
22	0.770	0.761	-0.009	1010.0	1062.4	52.4
18	0.900	0.896	-0.004	351	330.1	-20.9
13	0.930	0.934	0.004	206	205.0	-1.0
14	0.940	0.934	-0.006	195	204.8	9.8
39	0.970	0.970	0.000	113	117.4	4.4
23	0.970	0.969	-0.001	111	119.1	8.1
45	0.980	0.980	0.000	96.8	99.7	2.9
15	0.990	0.993	0.003	95.8	79.5	-16.3
50	0.980	0.980	0.000	95.7	99.7	4.0
44	0.980	0.980	0.000	95.2	99.6	4.4
46	0.980	0.981	0.001	94.0	98.6	4.6
71	0.980	0.979	-0.001	94.0	100.9	6.9
17	0.990	0.993	0.003	91.0	80.4	-10.6
74	0.990	0.993	0.003	89.0	80.1	-8.9
87	0.990	0.993	0.003	87.0	80.0	-7.0
73	0.990	0.993	0.003	83.0	80.1	-2.9
51	1.000	1.006	0.006	72.3	63.7	-8.6
49	1.000	1.006	0.006	68.4	64.1	-4.3
16	1.010	1.008	-0.002	59.3	61.3	2.0
38	1.020	1.024	0.004	55.5	47.5	-8.0
19	1.030	1.022	-0.008	44.0	49.3	5.3
20	1.030	1.036	0.006	35.0	39.4	4.4
75	1.050	1.051	0.001	33.0	32.0	-1.0
21	1.090	1.092	0.002	22.3	20.6	-1.7
40	1.090	1.093	0.003	22.0	20.3	-1.7
48	1.090	1.093	0.003	21.1	20.5	-0.6
47	1.090	1.092	0.002	19.9	20.5	0.6
41	1.130	1.132	0.002	15.9	15.0	-0.9
42	1.170	1.170	0.000	12.6	11.7	-0.9
43	1.210	1.207	-0.003	10.0	9.8	-0.2

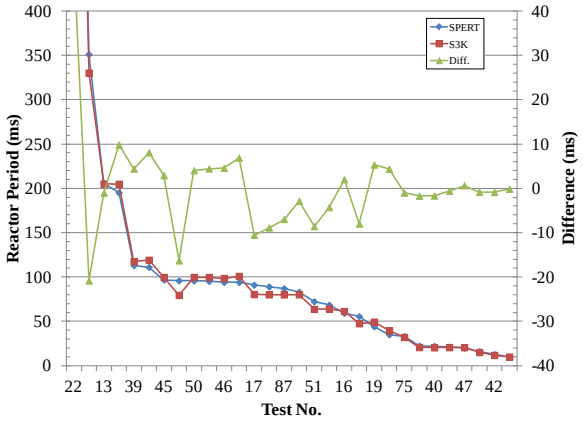

(a) Reactor period vs. test number

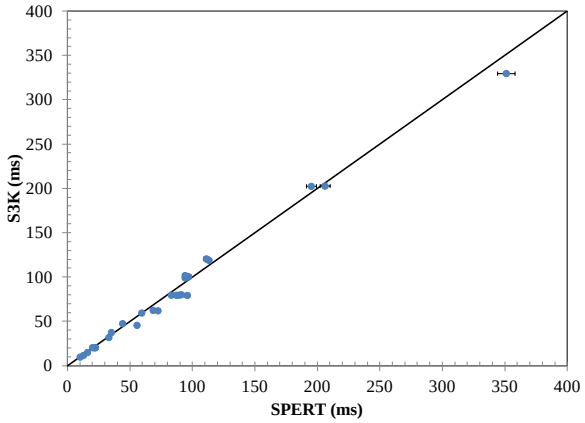

(b) Calculated vs. measured

Figure 4. Reactor period.

The reactor period is calculated with a bias of +0.5 ms and a standard deviation of 12 ms. Differences between the calculated and measured reactor periods are larger than the quoted experimental uncertainty (between 0.2 and 0.9 s for the super-prompt critical cases and up to 20 ms for the sub-prompt critical tests). However, note that cases with the same (experimental) initial reactivity insertion (e.g. tests 19 and 20) may differ as much as 10 ms in the (measured) reactor period. If one takes this fact into account, the agreement between calculated and measured reactor periods is reasonably good for the super-prompt critical cases. The reactor periods for the sub-prompt critical cases do not agree as well.

5.2. Maximum Reactor Power

Fig. 5 compares the experimental and calculated peak powers. Fig. 5-a shows measured (blue line) and calculated (red lines) peak powers as well as the differences (green line) for the different tests. The absolute differences between calculated and measured maximum reactor powers are below 20% in all cases. The experimental uncertainty is 15% [10].

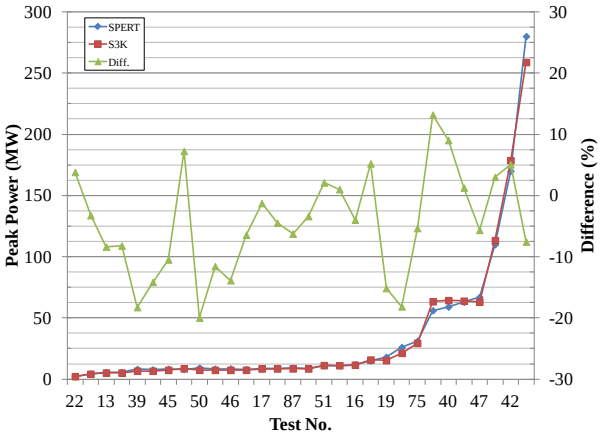

(a) Maximum reactor power vs. test number

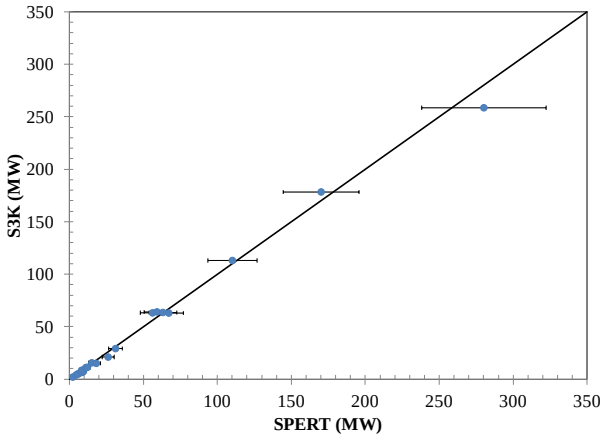

(b) Calculated vs. measured

Figure 5. Maximum reactor power.

As shown in Fig. 5, the calculated maximum reactor power is within the experimental uncertainty, except for tests 39, 50 and 20.

The following observations can be made:

- Sub-prompt critical cases (reactivity below 0.97$): The agreement between the calculated and measured maximum reactor power is good; differences are below 10%. Fig. 6-a compares the experimental (blue line) and calculated (red line) power evolutions for a typical sub-prompt critical case, namely Test 14, which has an inserted reactivity of 1.207$. Fig. 6-b compares the total reactivity. The power increase and the peak power are well predicted.

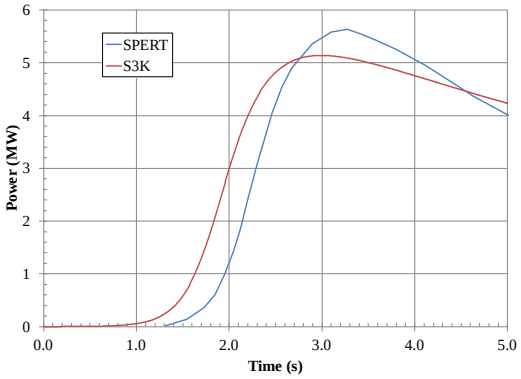

(a) Power

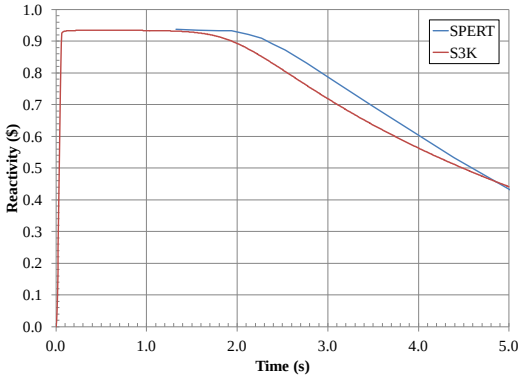

(b) Reactivity

Figure 6. Test 14: reactor power and reactivity. Inserted reactivity 0.934$.

- Super-prompt critical cases (reactivity above 1.03$): Absolute differences between calculated and measured peak powers are below 13%. Fig. 7-a compares the experimental and calculated power evolutions for a typical super-prompt critical case; namely Test 43, which has an inserted reactivity of 1.207$. Note that the power evolution is well predicted. Fig 7-b compares the total reactivity.

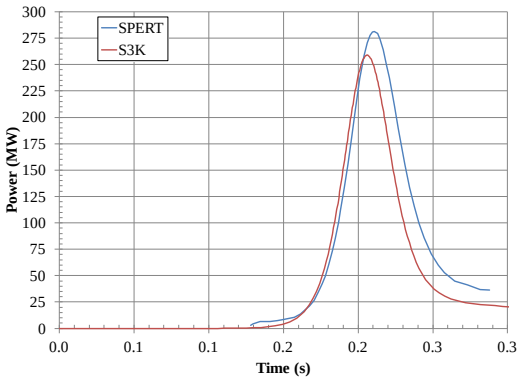

(a) Power

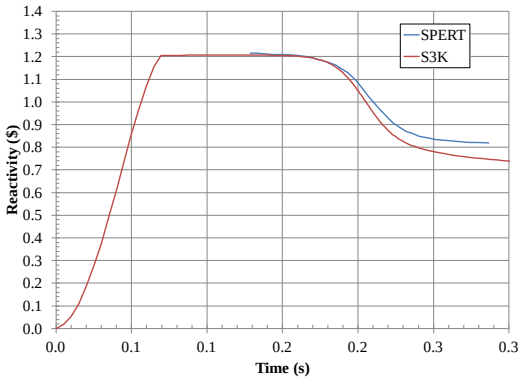

(b) Reactivity

Figure 7. Test 43: reactor power and reactivity. Inserted reactivity 1.207$.

- Cases close to prompt critical (reactivity between 0.97$ and 1.03$): The major discrepancies between calculated and measured peak powers are observed in this sub-set. Fig. 8-a compares the experimental and calculated power evolutions for Test 49, which has an inserted reactivity of 1.00$. Fig. 8-b compares the total reactivity. Measured and calculated power evolutions are in good agreement. The S3K solution probably rises faster because the inserted reactivity in the calculations is a little bit higher (1.006 $).

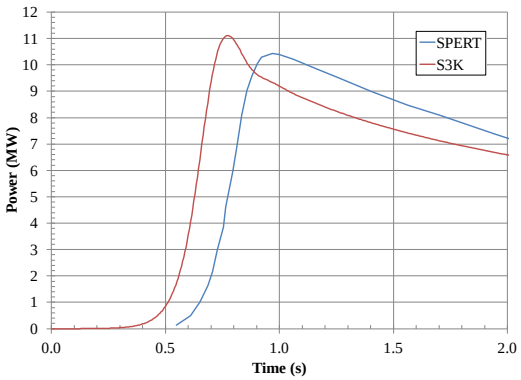

(a) Power

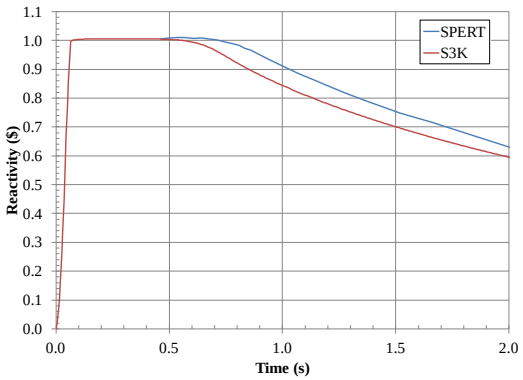

(b) Reactivity

Figure 8. Test 49: reactor power and reactivity. Inserted reactivity 1.006$.

5.3. Time to Peak Power

The time to peak power depends on the initial power (flux) level. Reference [10] does not provide the initial power level for each individual test. In the numerical simulations, all cases were run starting from the same power (50 W). No attempt was made to adjust the initial power to match the time to peak power. Fig. 9 compares the experimental and calculated time to peak power. It is clear that the numerical solution is not within the experimental uncertainty of the measurements except in a few cases.

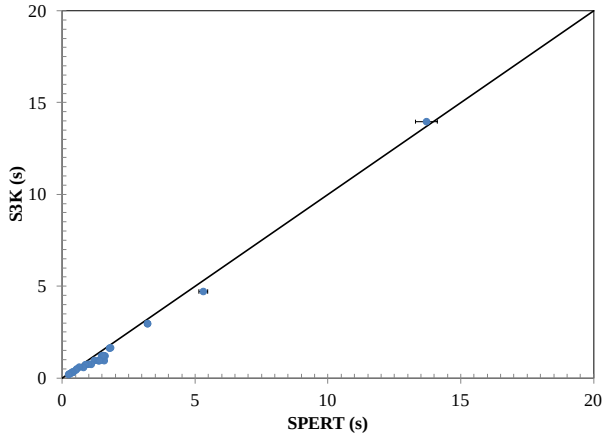

(a) Calculated vs. measured: all tests

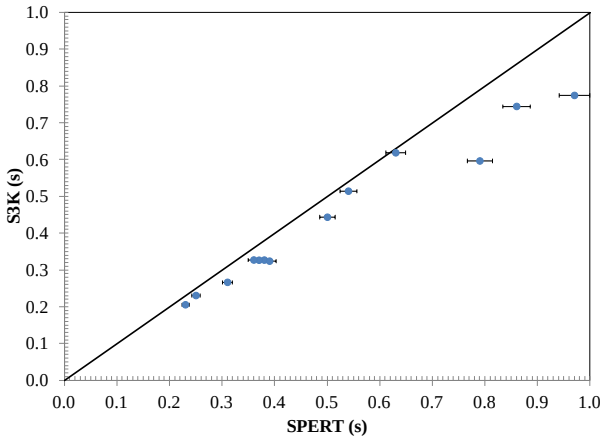

(b) Calculated vs. measured: prompt critical tests

Figure 9. Time to peak power.

5.4. Reactivity Compensation at Peak Power

Fig. 10 compares the experimental and calculated reactivity compensations. The bias is -0.007$ and the standard deviation is 0.024$. The reactivity compensation at peak power (i.e. the initial reactivity minus the reactivity at the time of the peak power) is a measure of the Doppler reactivity feedback for the cold start-up experiments.

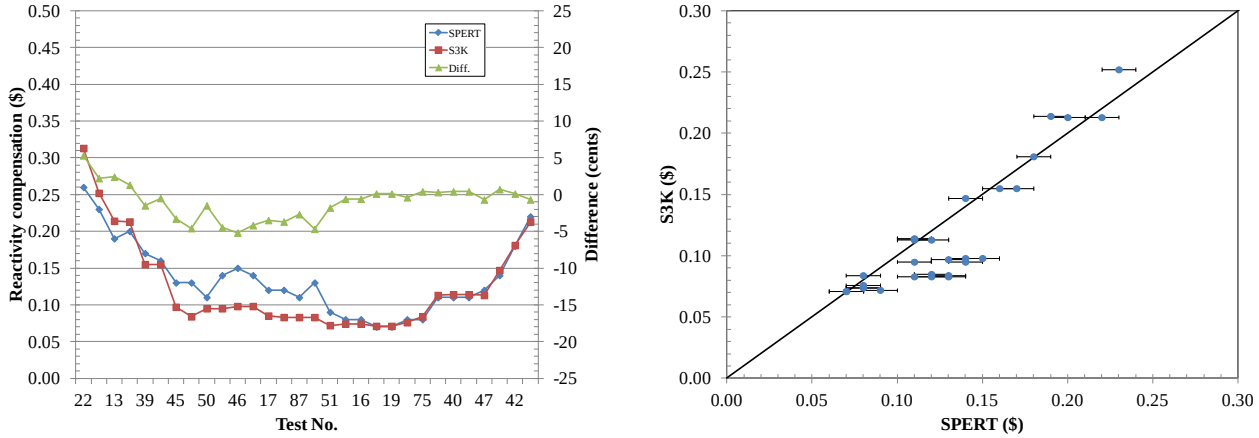

(a) Reactivity compensation vs. test number (b) Calculated vs. measured

Figure 10. Reactivity compensation.

The following observations can be made:

- Sub-prompt critical cases (reactivity below 0.97$): The agreement between the calculated and measured reactivity is reasonable; differences are between 0.02 $ and 0.05 $. Fig. 6-b compares the experimental and calculated reactivity evolutions for a typical sub-prompt critical case (Test 14). The reactivity evolution is reasonably predicted. After the peak power, the reactivity predicted by S3K decreases slower than in the measurements. The reason is still under investigation. Localized boiling may occur under low flow / low pressure conditions. Such conditions may be not well modeled by S3K.
- Super-prompt critical cases (reactivity above 1.03$): Absolute differences between calculated and measured compensated reactivity are below 0.007$. Fig. 7-b compares the experimental and calculated reactivity evolutions for a typical super-prompt critical case (Test 43).
- Cases close to prompt critical (reactivity between 0.97$ and 1.03$): The major differences between calculated and measured reactivity are observed in this sub-set. Fig. 8-b compares the experimental and calculated evolutions for Test 49, which has an inserted reactivity of 1.00$. Measured and calculated reactivity evolutions are in good agreement.

5.5. Key Results for the Prompt Critical Tests

Our main intention is to validate the Studsvik codes CASMO5 and S3K for RIA under prompt transient conditions. Table II and Fig. 11 compare the experimental and calculated peak power, energy release at the time of peak power and the reactivity compensation at the peak power time for Tests 75 – 43. These parameters are closely related to the fuel safety parameters in RIA applications (e.g. fuel enthalpy, prompt fuel enthalpy). Note that differences are within the experimental uncertainty.

Table II: Summary of results for prompt critical cases.

Test No.	Initial Reactivity	Peak Power			Energy Release			Reactivity Compensation		
	($)	(MW)			(MJ)			($)		
	SPERT	SPERT	S3K	Diff. (%)	SPERT	S3K	Diff.(%)	SPERT	S3K	Diff. ($)
75	1.050	31	29.3	-5.4	2.1	1.95	-7.7	0.08	0.08	0.004
21	1.090	56	63.4	13.2	2.8	2.68	-4.5	0.11	0.11	0.003
40	1.090	59	64.3	9.0	2.8	2.68	-4.5	0.11	0.11	0.004
48	1.090	63	63.8	1.3	2.8	2.70	-3.7	0.11	0.11	0.004
47	1.090	67	63.2	-5.7	3.0	2.67	-12.4	0.12	0.11	-0.007
41	1.130	110	113.3	3.0	3.8	3.52	-8.0	0.14	0.15	0.007
42	1.170	170	178.6	5.1	4.6	4.45	-3.4	0.18	0.18	0.001
43	1.210	280	258.8	-7.6	6.0	5.31	-13.0	0.22	0.21	-0.007

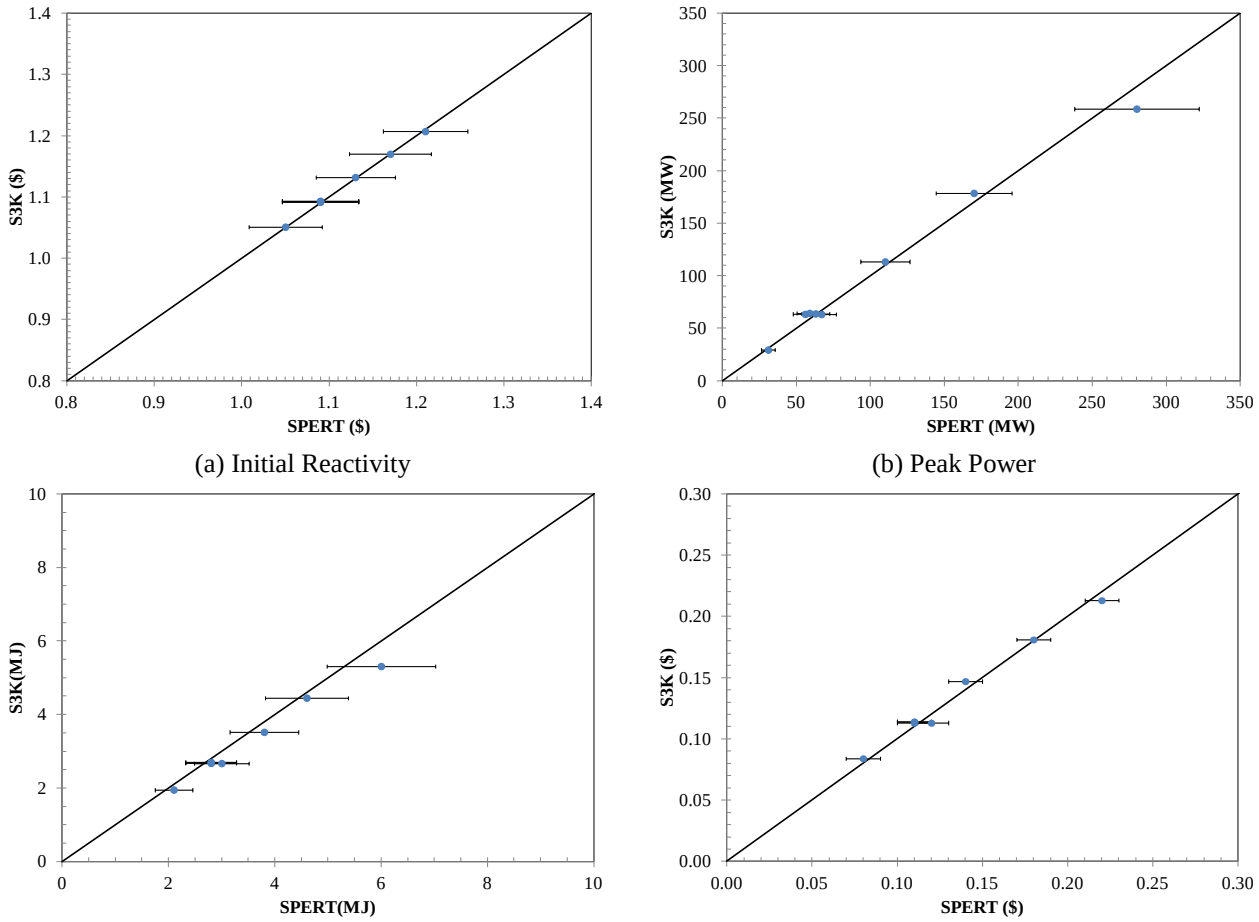

(a) Initial Reactivity

(b) Peak Power

(c) Energy Release

(d) Reactivity Compensation

Figure 11. Prompt critical cases: initial reactivity, peak power, energy release and reactivity compensation.

6. CONCLUSIONS

S3K provides a very flexible and accurate tool for RIA analysis as shown by the verification of S3K in a series of internationally recognized benchmarks [4–8]. The aim of the present work is to validate CASMO5 / SIMULATE-3K for RIA applications under super-prompt conditions using the feedback models recommended by Studsvik for LWR applications instead of the ones provided in the benchmark exercises.

For prompt critical transient conditions the following conclusions can be drawn:

- Maximum reactor powers are predicted with a bias of +1.6% and a standard deviation of 7.4%. Predicted and measured peak powers differ at most by 13%, which is within the experimental uncertainty (15 %) [10].
- Reactivity compensation at the time of the peak is predicted with a bias of +0.001$ and a standard deviation of 0.005$. Experimental and calculated values differ less than 0.01 $, which is within the experimental uncertainty (0.01–0.02 $).
- Energy released at the time of peak power is predicted with a bias of -7.1% and a standard deviation of 3.8%. Predicted and measured values differ at most by 13%. The experimental uncertainty is 17% [10].

In summary, this paper shows that there is good agreement between measured and calculated power related parameters for RIA transient in LWR under prompt transient cold start-up conditions.

The qualification against the SPERT III E-core tests is an ongoing activity within Studsvik. The results obtained for the cold start-up tests give us confidence to move towards the validation of CASMO5 / SIMULATE-3K against the hot start-up, hot standby and hot full power E-core experiments.

REFERENCES

1. L. Belblidia and G. Grandi, “SIMULATE-3K for Reactivity Insertion Accidents in LWR,” *Proceedings of PHYTRA 2 – The Second International Conference on Physics and Technology of Reactors and Applications*, Fez, Morocco, September 26-28, 2011, on CD-ROM, GMTR, Rabat, Morocco (2011).
2. G. Grandi and K. Smith, “SIMULATE-3K Explicit Fuel Pin Modelling in RIAs,” *Trans. Am. Nucl. Soc.*, **96**, 627, (2007).
3. J. L. Eller, “Application of SIMULATE-3K To PWR Reactivity Insertion Accident,” *Advances in Nuclear Fuel Management (ANFM 2009)*, Hilton Head Island, South Carolina, April 12-15, on CD-ROM, (2009).
4. H. Finnemann and A. Galati, “NEACRP 3D LWR Core Transient Benchmark,” Final Specification, NEACRP-L335 (Rev. 1), Nuclear Energy Agency Committee on Reactor Physics (January 1992).
5. J. Borkowski, J. Rhodes, P. Esser and K. Smith, “Three Dimensional Transient Capability in SIMULATE-3,” *Trans. Am. Nucl. Soc.*, **71**, 456, (1994).
6. R. Fraikin and H. Finnemann, “NEA-NSC 3-D/1D PWR Core Transient Benchmark Uncontrolled Withdrawal of Control Rods at Zero Power,” Final Specifications, NEA/NSC/DOC(93)9, OECD Nuclear Energy Agency (September 1993).
7. R. Fraikin, “PWR Benchmark of Uncontrolled Rods Withdrawal at Zero Power,” Final Report, NEA/NSC/DOC(96)30, OECD Nuclear Energy Agency (September 1997).
8. S. Langenbuch, W. Maurer and W. Werner, “Coarse-Mesh Nodal Diffusion Methods for the Analysis of Space-Time Effects in Large Light Water Reactors,” *Nucl. Sci. Eng.*, **63**, 437 (1977).
9. J. Dugone, “SPERT III Reactor Facility: E-core Revision,” IDO-17036, (November 1965).

10. R. K. McCardell, D. L. Herbon and J. E. Houghtaling, “Reactivity Accident Tests Results and Analyses for the SPERT III E-core a Small Oxide-Fueled, Pressurized Water Reactor,” IDO-17281, (March 1969).
11. L. A. Belblidia *et al.*, “SIMULATE-3K Peach Bottom 2 Turbine Trip 2 Benchmark Calculations,” *Nucl. Sci. Eng.*, **148**, 325 (2004).
12. G. Grandi *et al.*, “BWR Stability Analyses with SIMULATE-3K Benchmark Against Measured Plant Data,” *Progress in Nuclear Energy, DOI: 10.1016/j.pnucene.2010.03.002*.
13. J. Rhodes, K. Smith and D. Lee, “CASMO-5 Development and Applications,” *Advances in Nuclear Analysis and Simulation (PHYSOR 2006)*, Vancouver, BC, Canada, September 10-14, (2006).
14. G. Grandi *et al.*, “Effect of CASMO5 Cross Section Data and Doppler Temperature Definitions on LWR Reactivity Initiated Accidents,” *PHYSOR 2010 – Advances in Reactor Physics to Power the Nuclear Renaissance*, Pittsburgh, Pennsylvania, USA, May 9-14, (2010).

APPENDIX A: SPERT III E-Core Design Data Summary

General reactor design data	
Type	Experimental pressurized water reactor
Moderator / Coolant	H_2O / H_2O
Neutron energy	Thermal
Core type	Heterogeneous, rod type
Heat removal / Heat power	Plant 60 MW / Core 20 MW
Maximum coolant flow rate	1.2618 m^3/s
Design pressure and temperature	17.33 MPa at 616 K
Core design data	
Diameter	Approximately 66.04 cm
Active height	97.282 cm
Number of fuel assemblies	60
Fuel assemblies design data	
Number of assemblies	
25 rod assembly	48
16 rod assembly	4
CR assembly with fuel follower	8
Overall dimensions	
25 rod assembly	7.5565×7.5565×130.175 cm
16 rod assembly	6.3398×6.3398×130.175 cm
CR assembly with fuel followers	6.2890×6.2890×112.673 cm
Pitch	1.4859 cm
Flow area	
25 rod assembly	27.5086 cm^2
16 rod assembly	20.3871 cm^2
CR assembly with fuel follower	20.3871 cm^2
Fuel rods	
Type	Cylindrical
Materials	
Fuel tube	Stainless steel, type 348
Pellets	4.8 wt% enriched UO_2 (10.5 g/cm^3)
Gas gap	Helium
Rod outer diameter (cold)	1.1836 cm
Rod inner diameter (cold)	1.0820 cm
Fuel pellet diameter (cold)	1.0668 cm
Control rods	
Type	Upper section is absorber, lower section is fuel assembly
Composition	Absorber section 1.35 wt% ^{10}B in Type 18-8 stainless steel; 0.4724 cm thick hollow square box
Transient control rod	
Type	Cruciform; lower section absorber material; upper section stainless steel type 347
Number	1
Composition absorber section	1.35 w% 10B in a 18-8 stainless steel
Thickness of the blade	0.476 cm
Blade width	13.0175 cm
Absorber section length	96.52 cm
Acceleration during rod drop	50.8 m/s^2